Inorganic Chemistry

Article

One-Dimensional Polymers Containing Strictly Collinear Metal Ions: Synthesis and XRPD Characterization of Homoleptic Binary Metal Pyrazolates

Norberto Masciocchi,*,†,‡ G. Attilio Ardizzoia,*,†,§ Stefano Brenna,†,§ Girolamo LaMonica,†,§ Angelo Maspero,†,§ Simona Galli,†,‡ and Angelo Sironi‡,∥

Dipartimento di Scienze Chimiche, Fisiche e Matematiche, Università dell'Insubria, Via Valleggio 11, 22100 Como, Italy, Dipartimento di Chimica Strutturale e Stereochimica Inorganica, Università di Milano, Via Venezian 21, 20133 Milano, Italy, Dipartimento di Chimica Inorganica, Metallorganica ed Analitica, Università di Milano, Via Venezian 21, 20133 Milano, Italy, and Istituto di Scienze e Tecnologie Molecolari−CNR, Via Golgi 19, 20133 Milano, Italy

The synthesis of a number of 3d transition metal binary pyrazolates in microcrystalline form, thus suitable for a full XRPD characterization, has been pursued. The crystal and molecular structures of the $Fe(pz)_3$, $Co(pz)_2$, $Co(pz)_3$, and $Ni(pz)_2$ polymers, together with the few congeners reported in the recent literature, show that these species tend to afford highly crystalline materials where strictly collinear chains of metal atoms are present. Depending on the synthetic strategy used, $Ni(pz)_2$ has been found to crystallize as two different α (orthorhombic) and β (monoclinic) phases, possessing nearly identical intramolecular features. Data for each compound follow. $Fe(pz)_3$: $C_9H_9FeN_6$, hexagonal, $P6_3/m$, $a = 9.1745(3)$ Å, $c = 7.2191(4)$ Å, $Z = 2$. $Co(pz)_2$: $C_6H_6CoN_4$, orthorhombic, *Ibam*, $a = 7.5239(5)$ Å, $b = 14.3461(9)$ Å, $c = 7.4331(5)$ Å, $Z = 4$. $Co(pz)_3$: $C_9H_9CoN_6$, hexagonal, $P6_3/m$, $a = 9.1966(3)$ Å, $c = 7.1051(3)$ Å, $Z = 2$. α-$Ni(pz)_2$: $C_6H_6N_4Ni$, orthorhombic, *Cmcm*, $a = 16.6758(11)$ Å, $b = 6.4872(4)$ Å, $c = 6.9423(6)$ Å, $Z = 4$. β-$Ni(pz)_2$: $C_6H_6N_4Ni$, monoclinic, $P2_1/m$, $a = 9.967(2)$ Å, $b = 6.975(1)$ Å, $c = 6.016(1)$, Å, $\beta = 98.50(1)°$, $Z = 2$. The thermal stability and the detailed structural properties of these model compounds have been evaluated, in the light of the technologically relevant crystal phases (the well-known metal-diazolates showing reversible spin-crossover or spin-transition behavior) obtainable upon doping, magnetic dilution, and ring substitution (in the 4-position).

Introduction

The synthesis and characterization of polymeric species containing transition metals and organic fragments have recently attracted the interest of several groups aiming to develop materials in which the peculiar properties of the metal ions employed can be finely tuned by minor modifications of the organic moiety. Among these "hybrid organic−inorganic" species, one-dimensional chains with transition metals in their backbones[1] have been largely studied because of their anisotropic structures, which can lead, in the most fortunate cases, to materials bearing relevant technological properties, such as, for example, magnetism,[2] conductivity,[3] luminescence,[4] and NLO activity.[5] Among the properties which might have a considerable technological impact, spin-

* To whom correspondence should be addressed. E-mail: norberto.masciocchi@uninsubria.it (N.M.); ardizzoia@uninsubria.it (G.A.A.).
  † Università dell'Insubria.
  ‡ Dipartimento di Chimica Strutturale e Stereochimica Inorganica, Università di Milano.
  § Dipartimento di Chimica Inorganica, Metallorganica ed Analitica, Università di Milano.
  ∥ Istituto di Scienze e Tecnologie Molecolari−CNR.

(1) Nguyen, P.; Gómez-Elipe, P.; Manners, I. *Chem. Rev.* **1999**, *99*, 1515−1548.
(2) Miller, J. S. *Inorg. Chem.* **2000**, *39*, 4392−4408. Ribas, J.; Escuer, A.; Monfort, M.; Vicente, R.; Cortés, R.; Lezama, L.; Rojo, T.; Goher, M. A. S. In *Magnetism: Molecules to Materials II*; Miller, J. S., Drillon, M., Eds.; Wiley-VCH: Weinheim, 2001.
(3) Xenikos, D. G.; Müller, H.; Jouan, C.; Sulpice, A.; Tholence, J. L. *Solid State Commun.* **1997**, *102*, 681−685. Cerrada, E.; Diaz, M. C.; Diaz, C.; Laguna, M.; Sabater, A. *Synth. Met.* **2001**, *119*, 91−92.
(4) Shieh, S. J.; Hong, X.; Peng, S. M.; Che, C. M. *J. Chem. Soc., Dalton Trans.* **1994**, 3067−3068. Parsons, S.; Pikramenou, Z.; Solan, G. A.; Winpenny, R. E. P. *J. Cluster Sci.* **2000**, *11*, 227−232. Ciurtin, D. M.; Pschirer, N. G.; Smith, M. D.; Bunz, U. H. F.; zur Loye, H.-C. *Chem. Mater.* **2001**, *13*, 2743−2745.
(5) Thompson, M. E.; Chiang, W. C.; Myers, L. K.; Langhoff, C. A. In *Nonlinear Optics and Materials*; Cantrell, C. D., Ed.; SPIE Proceedings: Bellingham, WA, 1991; Vol. 1497, pp 423−429.

crossover (SC) and spin-transition (ST) behaviors and valence tautomerism (VT) of magnetic ions in polynuclear systems hold a relevant position, because molecular bistability[6] and thermally (or otherwise) induced hysteresis loops[7] may be employed in a number of processes and devices, ranging from data elaboration and information storage,[8] to color displays,[9] temperature and pressure sensors,[10] and generation of phase holograms.[11]

Several polymeric systems showing SC or ST at, or near, room temperature have been synthesized and spectroscopically, thermally, and magnetically characterized; among others, Fe(II)-complexes, bridged by polyazaheterocycles, appeared as versatile and promising compounds.[9b,12] Accordingly, these types of materials are currently being assessed by industrial organizations for possible practical applications.[12] In these systems, the cooperativity of subtle effects, the *collinear* geometry of the active centers, and the rigidity of the whole one-dimensional framework greatly enhance (by electron−phonon coupling) their magnetic response, spin-transition features,[13] and even photomechanical effects.[14] However, their chemical and thermal stability is limited by the presence of counterions, balancing, in the solid state, the net positive charges of the $[(FeL_3)^{2+}]_n$ chains. Moreover, their structural characterization has been typically revealed as problematic, because they generally afford poorly crystalline materials[15] and tend to behave very differently as a result of even small differences in preparation.[8,9a] Thus, their structures have been mostly inferred by indirect evidence, such as IR, Raman, Mössbauer, and EXAFS spectroscopy or structure analysis of the corresponding oligomeric species[16] or of vaguely related polymers.[17] Only recently, the crystal structures of the bispyrazolate-iron(II)[18] and bis(1-methyl-2-thioimidazolate)iron(II)[19] polymers, containing tetrahedral d^6 ions, have been reported and correlated to their magnetic properties.

With the aim of preparing crystalline samples containing neutral chains with the ML_n formulation ($n = 2, 3$; L = a negatively charged *exo*-bidentate group), possessing much higher thermal stability than the already known species containing neutral heterocycles, we have investigated the synthesis and the thermal stability of Fe(III), Co(II), Co(III), and Ni(II) pyrazolates, together with their detailed structures, as determined from X-ray powder diffraction (XRPD) methods.[20] In the recent past, these methods have been successfully employed to characterize a number of analogous species, such as Cu, Ag, Zn, Cd, and Hg pyrazolates,[21] Cu and Ag imidazolates,[22] and Co, Ni, Cu, Zn, and Ag pyrimidin-2-olates.[23]

The results presented hereafter, although lacking important magnetic investigations, are likely to influence the development of suitable materials once the control of the stereochemistry at the metals and their nature and variety are taken in consideration (for example, by tuning the structural and electronic properties of mixed-metal, mixed-valence, or magnetically diluted species derived from the end-members described later).

Experimental Section

General Methods. Pyrazole (Hpz) and metal salts were used as supplied (Aldrich Chemical Co.). Solvents were purified by standard methods. Infrared spectra were recorded on a Bio-Rad FTIR 7 instrument. Thermogravimetric and calorimetric analyses were performed on a Perkin-Elmer TGA7 system and DSC7 calorimeter. Elemental analyses (C, H, N) were carried out at the Microanalytical Laboratory of the University of Milan.

Synthesis of Iron(III) and Cobalt(III) Pyrazolates. Fe(pz)₃ and Co(pz)₃ have been prepared following a similar synthetic route: Fe(acac)₃ (0.70 g, 1.98 mmol) or Co(acac)₃ (0.70 g, 1.97 mmol) and pyrazole (2.00 g, metal/Hpz ratio 1/15) were heated in a sealed flask under nitrogen for 6 h at 180 °C without stirring. The mixture was then allowed to cool and solidify giving a brick-red (iron) or pale brown (cobalt) solid. The residue was then washed with acetone (50 mL) in order to remove excess pyrazole and then filtered off, giving 0.491 g, 96.6% and 0.485 g, 94.7% of Fe(pz)₃ and Co(pz)₃, respectively. IR (cm⁻¹) Fe(pz)₃: 1275 m, 1181 s, 1165 m, 1064 s, 885 w, 754 s, 721 w, 629 m. Anal. Calcd for $C_9H_9FeN_6$: C, 42.05%; H, 3.53%; N, 32.69%. Found: C, 42.17%; H, 3.58%; N, 32.67%. IR (cm⁻¹) Co(pz)₃: 1286 m, 1190 m, 1178 w, 1069 s, 883 w, 748 s, 722 w, 632 w. Anal. Calcd for $C_9H_9CoN_6$: C, 41.55%; H, 3.49%; N, 32.31%. Found: C, 41.58%; H, 3.53%; N, 32.37%.

(6) Kahn, O.; Launay, J. P. *Chemtronics* **1988**, *3*, 140−151.
(7) Kröber, J.; Codjovi, E.; Kahn, O.; Grolière, F.; Jay, C. *J. Am. Chem. Soc.* **1993**, *115*, 9810−9811.
(8) Zarembowitch, J.; Kahn, O. *New. J. Chem.* **1991**, *15*, 181−190.
(9) Kahn, O.; Kröber, J.; Jay, C. *Adv. Mater.* **1992**, *4*, 718−728. Garcia, Y.; van Koningsbruggen, P.; Codjovi, E.; Lapouyade, R.; Kahn, O.; Rabardel, L. *J. Mater. Chem.* **1997**, *7*, 857−858.
(10) Roubeau, O.; Haasnoot, J. G.; Codjovi, E.; Varret, F.; Reedijk, J. *Chem. Mater.* **2002**, *14*, 2558−2566.
(11) Hauser, A. *Coord. Chem. Rev.* **1991**, *111*, 275−290.
(12) Gütlich, P.; Garcia, Y.; Goodwin, H. A. *Chem. Soc. Rev.* **2000**, *29*, 419−427.
(13) van Koningsbruggen, P. J.; Garcia, Y.; Codjovi, E.; Lapouyade, R.; Kahn, O.; Fournès, L.; Rabardel, L. *J. Mater. Chem.* **1997**, *7*, 2069−2075.
(14) Jung, O.-S.; Pierpont, C. G. *J. Am. Chem. Soc.* **1994**, *116*, 2229−2230. Jung, O.-S.; Lee, Y.-A.; Pierpont, C. G. *Synth. Met.* **1995**, *71*, 2019−2020.
(15) Smit, E.; Manoun, B.; Verryn, S. M. C.; de Waal, D. *Powder Diffr.* **2001**, *16*, 37−41.
(16) (a) Vos, J. G.; Groeneveld, W. L. *Inorg. Chim. Acta* **1977**, *23*, 123−126. (b) Vos, J. G.; le Fêbre, R. A.; de Graaff, R. A. G.; Haasnot, J. G.; Reedijk, J. *J. Am. Chem. Soc.* **1983**, *105*, 1682−1685. (c) Garcia, Y.; van Koningsbruggen, P. J.; Bracic, G.; Guionneau, P.; Chasseau, D.; Cascarano, G. L.; Moscovici, J.; Lambert, K.; Michalowicz, A.; Kahn, O. *Inorg. Chem.* **1997**, *36*, 6357−6365. Michalowicz, A.; Moscovici, J.; Charton, J.; Sandid, F.; Benamrane, F.; Garcia, Y. *J. Synchrotron Radiat.* **2001**, *8*, 701−703.
(17) van Koningsbruggen, P. J.; Garcia, Y.; Kahn, O.; Fournès, L.; Koijman, H.; Spek, A.; Haasnoot, J. G.; Moscovici, J.; Provost, K.; Michalowicz, A.; Renz, F.; Gütlich, P. *Inorg. Chem.* **2000**, *39*, 1891−1900.
(18) Patrick, B. O.; Reiff, W. M.; Sánchez, V.; Storr, A.; Thompson, R. C.; *Polyhedron* **2001**, *20*, 1577−1585.

(19) Rettig, S. J.; Sánchez, V.; Storr, A.; Thompson, R. C.; Trotter, J. *Inorg. Chem.* **1999**, *38*, 5920−5923.
(20) Masciocchi, N.; Sironi, A. *J. Chem. Soc., Dalton Trans.* **1997**, 4643−4650.
(21) (a) Masciocchi, N.; Moret, M.; Cairati, P.; Sironi, A.; Ardizzoia, G. A.; La Monica, G.; Cenini, S. *J. Am. Chem. Soc.* **1994**, *116*, 7668−7676. (b) Masciocchi, N.; Ardizzoia, G. A.; Maspero, A.; La Monica, G.; Sironi, A. *Inorg. Chem.* **1999**, *38*, 3657−3664.
(22) (a) Masciocchi, N.; Moret, M.; Cairati, P.; Sironi, A.; Ardizzoia, G. A.; La Monica, G. *J. Chem. Soc., Dalton Trans.* **1995**, 1671−1675. (b) Masciocchi, N.; Bruni, S.; Cariati, E.; Cariati, F.; Galli, S.; Sironi, A. *Inorg. Chem.* **2001**, *40*, 5897−5905.
(23) Masciocchi, N.; Corradi, E.; Moret, M.; Ardizzoia, G. A.; Maspero, A.; La Monica, G.; Sironi, A. *Inorg. Chem.* **1997**, *36*, 5648−5650. Masciocchi, N.; Ardizzoia, G. A.; La Monica, G.; Maspero, A.; Sironi, A. *Angew. Chem., Int. Ed.* **1998**, *37*, 3366−3369.

Synthesis of Cobalt(II) Pyrazolate. To a degassed solution of Co(CH₃COO)₂·4H₂O (0.50 g, 2.00 mmol) in *n*-butanol (20 mL) was added pyrazole (0.546 g, 8.00 mmol) under stirring. The purple solution was heated at 130 °C for 5 h. During this time, a deep-violet solid formed. The solid was filtered under an atmosphere of dry dinitrogen, washed with hot *n*-butanol (20 mL) and methanol (10 mL), and then dried under vacuum (0.328 g, 85%). IR (cm⁻¹): 1294 m, 1262 w, 1187 s, 1071 s, 926 m, 871 w, 743 s, 627 m. Anal. Calcd for $C_6H_6CoN_4$: C, 37.33%; H, 3.13%; N, 29.02. Found: C, 37.12%; H, 3.21%; N, 29.16%.

Synthesis of Nickel(II) Pyrazolate (α-Phase). (a) To a solution of Ni(CH₃COO)₂·4H₂O (0.80 g, 3.22 mmol) in *n*-butanol (25 mL) was added pyrazole (0.876 g, 12.9 mmol) under stirring. The green solution was heated at 130 °C for 4 h. During this time, a yellow solid formed. The solid was filtered off, washed with hot *n*-butanol (20 mL) and methanol (10 mL), and then dried under vacuum. (0.565 g, 91%). (b) Ni(CH₃COO)₂·4H₂O (0.70 g, 2.81 mmol) and pyrazole (2.87 g, Ni/Hpz ratio 1/15) were heated in a sealed flask under nitrogen for 5 h at 180 °C without stirring. The mixture was then allowed to cool and solidify giving a yellow solid. The residue was then washed with acetone (50 mL) in order to remove excess pyrazole and then filtered, giving 0.527 g, 97.3%. The α-phase was also obtained employing Ni(acac)₂ or Ni(OH)₂ in place of Ni(CH₃COO)₂. IR (cm⁻¹): 1284 m, 1190 s, 1188 m, 1177 w, 1066 s, 883 w, 769 s, 746 s, 668 m, 634 w. Anal. Calcd for $C_6H_6N_4Ni$: C, 37.37%; H, 3.14%; N, 29.05%. Found: C, 37.41%; H, 3.22%; N, 29.12%.

Synthesis of Nickel(II) Pyrazolate (β-Phase). NiO (0.20 g, 2.68 mmol) and pyrazole (2.77 g, Ni/Hpz ratio 1/15) were heated in a sealed flask under nitrogen for 12 h at 180 °C under smooth stirring. The mixture was allowed to cool and solidify giving a brown-yellow solid. The residue was then washed with acetone (50 mL) and filtered obtaining β-Ni(pz)₂, contaminated by variable amounts of α-Ni(pz)₂ (typically in the 10−20% range, XRPD evidence) and some NiO. Accordingly, no reliable elemental analysis could ever be obtained. No significant differences between the IR spectra of the pure α-phase and the samples rich in β-phase were observed (apart from a small broadening of the main absorptions), thus suggesting nearly identical "intramolecular" features.

X-ray Powder Diffraction Analysis of Fe(pz)₃, Co(pz)₂, Co(pz)₃, α-Ni(pz)₂ and β-Ni(pz)₂. The powders were gently ground in an agate mortar and then cautiously deposited in the hollow of an aluminum holder equipped with a zero background plate (supplied by The Gem Dugout, State College, PA). Diffraction data (Cu Kα, λ = 1.5418 Å) were collected on a vertical scan Philips PW1820 diffractometer, equipped with Soller slits, a secondary beam curved graphite monochromator, a Na(Tl)I scintillation detector, and pulse height amplifier discrimination. The generator was operated at 40 kV and 40 mA. Slits used: divergence 1.0°, antiscatter 1.0°, and receiving 0.2 mm. Nominal resolution for the present setup is 0.12° 2θ (fwhm) for the Si(111) peak at 28.44° (2θ). Long overnight scans were performed with 5° < 2θ < 105° [Fe(pz)₃, Co(pz)₂, Co(pz)₃, and α-Ni(pz)₂] and 5° < 2θ < 75° [β-Ni(pz)₂], with *t* = 10 s and Δ2θ = 0.02°. The low angle sections of the collected data sets are shown in Figure 1.

For Fe(pz)₃, α-Ni(pz)₂, and β-Ni(pz)₂, indexing was obtained with the aid of TREOR[24] (figures of merit in Table 1). Systematic absences indicated *P*6₃/*m*, *Cmcm*, and *P*2₁/*m* as the probable space groups, respectively, later confirmed by successful solution and refinement. Visual inspection suggested the strict
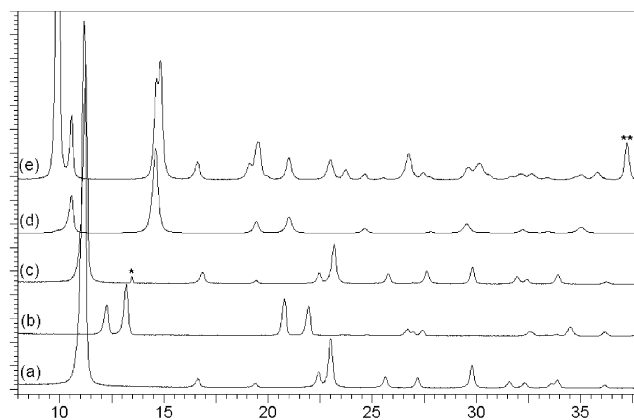

Figure 1. Low angle sections of the raw data for (a) Fe(pz)₂, (b) Co(pz)₂, (c) Co(pz)₃, (d) α-Ni(pz)₂, and (e) β-Ni(pz)₂ [partially contaminated by α-Ni(pz)₂]. * indicates spurious peak from sample holder; ** indicates contaminating NiO (see text). Vertical scale, diffracted intensity in arbitrary units; horizontal scale, 2θ, deg.

isomorphous character of Co(pz)₃ with Fe(pz)₃, and that of Co(pz)₂ with Zn(pz)₂.[21b] Structure solutions of Fe(pz)₃, α-Ni(pz)₂, and β-Ni(pz)₂ were initiated by EXPO,[25] which afforded all metal locations as well as the position of a few other light atoms. With the help of difference Fourier syntheses and geometrical modeling, approximate coordinates for the remaining non-hydrogen atoms were later obtained. The final refinements were performed with the aid of the GSAS suite of programs,[26] by imposing steric restraints to the rigid pyrazolate rings, which were idealized with average literature values [1,2-distances, 1.38(1) Å; 1,3-distances, 2.23(1) Å]. The peak shapes were best described by the Thompson/Cox/Hastings formulation[27] of the pseudo-Voigt function, with GV and LY set to zero. The experimental background was modeled by a cosine Fourier series while systematic errors were modeled with the aid of sample-displacement angular shifts and preferred orientation corrections in the March−Dollase[28] formulation. Metal atoms were given a refinable isotropic displacement parameter [$U_{iso}(M)$], while lighter atoms' *U* values were arbitrarily given [$U_{iso}(M) + 0.02$] Å² values. The contribution of the hydrogen atoms to the scattered intensity was neglected. Because β-Ni(pz)₂ could not be prepared as a monophasic sample, its structural model was refined on a complex XRPD pattern, affected by the contaminating α-Ni(pz)₂ and nickel(II) oxide phases; therefore, it required the extensive use of soft restraints [based on the known refined values for α-Ni(pz)₂] to maintain a chemically plausible stereochemistry. Accordingly, the derived geometry, in the following, will not be discussed in detail; nevertheless, main structural features, such as chain conformation, intermetallic Ni···Ni distances, and packing motif, are clearly established. Scattering factors, corrected for real and imaginary anomalous dispersion terms, were taken from the internal library of GSAS. Final R_p, R_{wp}, and R_F agreement factors, together with details on the data collections and analyses for the five crystal phases, can be found in Table 1. Relevant structural parameters are gathered in Table 2. Figure 2 shows the final

(24) Werner, P. E.; Eriksson, L.; Westdahl, M. *J. Appl. Crystallogr.* **1985**, *18*, 367−370.

(25) Altomare, A.; Burla, M. C.; Cascarano, G.; Giacovazzo, G.; Guagliardi, A.; Moliterni, A. G. G.; Polidori, G. *J. Appl. Crystallogr.* **1995**, *28*, 842−846. Altomare, A.; Burla, M. C.; Camalli, M.; Carrozzini, B.; Cascarano, G. L.; Giacovazzo, G.; Guagliardi, A.; Moliterni, A. G. G.; Polidori, G.; Rizzi, R. *J. Appl. Crystallogr.* **1999**, *32*, 339−340.

(26) Larson, A. C.; Von Dreele, R. B. *LANSCE*, MS-H805; Los Alamos National Laboratory: Los Alamos, NM, 1990.

(27) Thompson, P.; Cox, D. E.; Hastings, J. B. *J. Appl. Crystallogr.* **1987**, *20*, 79−83.

(28) March, A. *Z. Kristallogr.* **1932**, *81*, 285−297. Dollase, W. A. *J. Appl. Crystallogr.* **1987**, *19*, 267−272.

Table 1. Crystal Data and Details on Refinement for Compounds Fe(pz)₃, Co(pz)₂, Co(pz)₃, α-Ni(pz)₂ and β-Ni(pz)₂[a]

	Fe(pz)₃	Co(pz)₂	Co(pz)₃	α-Ni(pz)₂	β-Ni(pz)₂
indexing method	TREOR[24]	TREOR	TREOR	TREOR	TREOR
indexing FOMs	20, 80, 100	na	na	13, 18, 2	19, 28, 43
N, M,[43] F[44]	(0.008, 26)			(0.015, 42)	(0.013, 34)
syst	hexagonal	orthorhombic	hexagonal	orthorhombic	monoclinic
space group	$P6_3/m$	$Ibam$	$P6_3/m$	$Cmcm$	$P2_1/m$
a, Å	9.17454(33)	7.5239(5)	9.19657(31)	16.6758(11)	8.9673(18)
b, Å	9.17454(33)	14.3461(9)	9.19657(31)	6.4872(4)	6.9752(13)
c, Å	7.2191(4)	7.4331(5)	7.10514(30)	6.9423(6)	6.0158(14)
α, deg	90	90	90	90	90
β, deg	90	90	90	90	98.502(12)
γ, deg	120	90	120	90	90
Z	2	4	2	4	2
fw, g mol⁻¹	257.06	187.03	260.14	192.85	192.85
V, Å³	526.24(4)	802.31(9)	520.42(3)	751.01(9)	372.17(13)
D_{calcd}, g cm⁻³	1.622	1.598	1.660	1.707	1.720
$F(000)$	262	388	264	392	196
μ(Cu Kα), cm⁻¹	113.99	171.03	134.09	31.60	31.87
T, K	298(2)	298(2)	298(2)	298(2)	298(2)
2θ range, °	15−105	11−100	15−105	17−105	14−75
N_{data}	4500	4450	4500	4400	3050
N_{obs}	235	236	230	257	344
R_p, R_{wp}[c]	0.067, 0.083	0.071, 0.093	0.067, 0.084	0.082, 0.107	0.105, 0.134
R_F[c]	0.125	0.129	0.109	0.115	0.153

[a] Estimated standard deviation values in parentheses. [b] FOMs = figures of merit; na = not applicable. [c] $R_p = \sum_i |y_{i,o} - y_{i,c}|/\sum_i |y_{i,o}|$, $R_{wp} = [\sum_i w_i (y_{i,o} - y_{i,c})^2/\sum_i w_i (y_{i,o})^2]^{1/2}$, $R_F = \sum_n ||F_{n,o}| - |F_{n,c}||/\sum_i |F_{n,o}|$, where $y_{i,o}$ and $y_{i,c}$ are the observed and calculated profile intensities, respectively, while $|F_{n,o}|$ and $|F_{n,c}|$ are the observed and calculated structure factors. The summations run over i data points or n independent reflections. Statistical weights w_i are normally taken as $1/y_{i,o}$.

Table 2. Relevant Structural Parameters for Polymeric M(pz)ₙ Species (M = 3d Transition Metal; esd's in Parentheses)

	Fe(pz)₂[18]	Fe(pz)₃	Co(pz)₂	Co(pz)₃	α-Ni(pz)₂	β-Ni(pz)₂	Cu(pz)₂[21b]	Zn(pz)₂[21b]
syst	orthorhombic	hexagonal	orthorhombic	hexagonal	orthorhombic	monoclinic	orthorhombic	orthorhombic
space group	$Ibam$	$P6_3/m$	$Ibam$	$P6_3/m$	$Cmcm$	$P2_1/m$	$Ibam$	$Ibam$
a, Å	7.515(2)	9.174[a]	7.524[a]	9.196[a]	16.676[a]	8.967	7.917(1)	7.4829(4)
b, Å	14.604(4)	9.174	14.346	9.196	6.487	**6.975**	11.491(2)	14.3844(6)
c, Å	**7.359(1)**	**7.219**	7.433	**7.105**	**6.942**	6.016	**7.778(1)**	**7.3831(3)**
α, deg	90	90	90	90	90	90	90	90
β, deg	90	90	90	90	90	98.49	90	90
γ, deg	90	120	90	120	90	90	90	90
M site sym	222	3̄	222	3̄	2/m	1̄	222	222
Pz site sym	m	m	m	m	m	m	m	m
M···M, Å	3.68	3.6095(2)	3.7165(3)	3.5526(2)	3.4711(3)	3.488(1)	3.89	3.69
M−N, Å	2.027(1)	1.979(2)	2.006(3)	1.952(3)	1.869(3)	1.888(2), 1.886(2)[d]	1.957(2)	1.970(7)
N−M−N, deg	108.93(9)	88.64(7)	106.0(4)	87.98(8)	88.75(15)	88.3(4)[d]	94.3(1)	108.0(3)
	109.22(6)	91.36(7)	108.8(1)	92.02(8)	91.25(15)	91.7(4)	99.4(1)	109.6(5)
	110.27(6)	180	113.7(5)	180	180	180	139.5(1)	110.9(5)
chains pack	hexagonal[b]	hexagonal	hexagonal[b]	hexagonal	hexagonal[b]	rectangular[b]	hexagonal[b]	hexagonal[b]
color (RT)	red-brown	brown	purple	beige	yellow	yellow	green	colorless
T_{dec}, °C	na	300	450	450	420	>400	270	441
$|\epsilon|$[c]	0.0927	0	0.0765	0	0.4634		0.1187	0.0827

[a] Actual values and their esd's are reported in Table 1. [b] Idealized packing symmetry. [c] $\epsilon = 1 - [(a^2 + b^2)/a^2]^{1/2}/2$ (or equivalent, after proper axis transformation). [d] Because of the polyphasic nature of the sample, an extensive use of geometrical restraints was needed (see text). Bold characters highlight the polymeric chain axis.

Rietveld refinement plots. Final fractional coordinates are supplied as Supporting Information. Crystallographic data (excluding structure factors) for the structures reported in this paper have been deposited with the Cambridge Crystallographic Data Centre as supplementary publication nos. CCDC 188326−188330. Copies of the data can be obtained free of charge on application to CCDC, 12 Union Road, Cambridge CB2 1EZ, UK (Fax: (+44) 1223 336-033. E-mail: deposit@ccdc.cam.ac.uk.).

Results

Syntheses. Binary metal pyrazolates of oxidatively stable metal ions can be generally obtained quite easily by simple reaction of the corresponding metal salts (usually chlorides or nitrates) with pyrazole in aqueous basic medium.[16,29]

Following this route, nickel(II) and cobalt(II) metal pyrazolates have been prepared in the last years and have been the matter of detailed spectroscopic and magnetic studies.[30,31] As early as 1968, the syntheses of both iron(II) and iron(III) pyrazolates were described,[32] by reacting directly organometallic precursors, such as [CpFe(CO)₂]₂ or [CpFe-(CO)₂Cl], with pyrazole in toluene. In addition, the synthesis

(29) (a) Bagley, M. J.; Nicholls, D.; Warburton, B. A. *J. Chem. Soc. A* **1970**, 2694−2697. (b) Ehlert, M. K.; Storr, A.; Thompson, R. C. *Can. J. Chem.* **1993**, *71*, 1412−1424.
(30) Blake, A. B.; Ewing, D. F.; Hamlin, J. E.; Lockyer, J. M. *J. Chem. Soc., Dalton Trans.* **1977**, 1897−1901.
(31) Storr, A.; Summers, D. A.; Thompson, R. C. *Can. J. Chem.* **1998**, *76*, 1130−1137.
(32) Seel, F.; Sperber, V. *Angew. Chem., Int. Ed. Engl.* **1968**, *7*, 70−71.
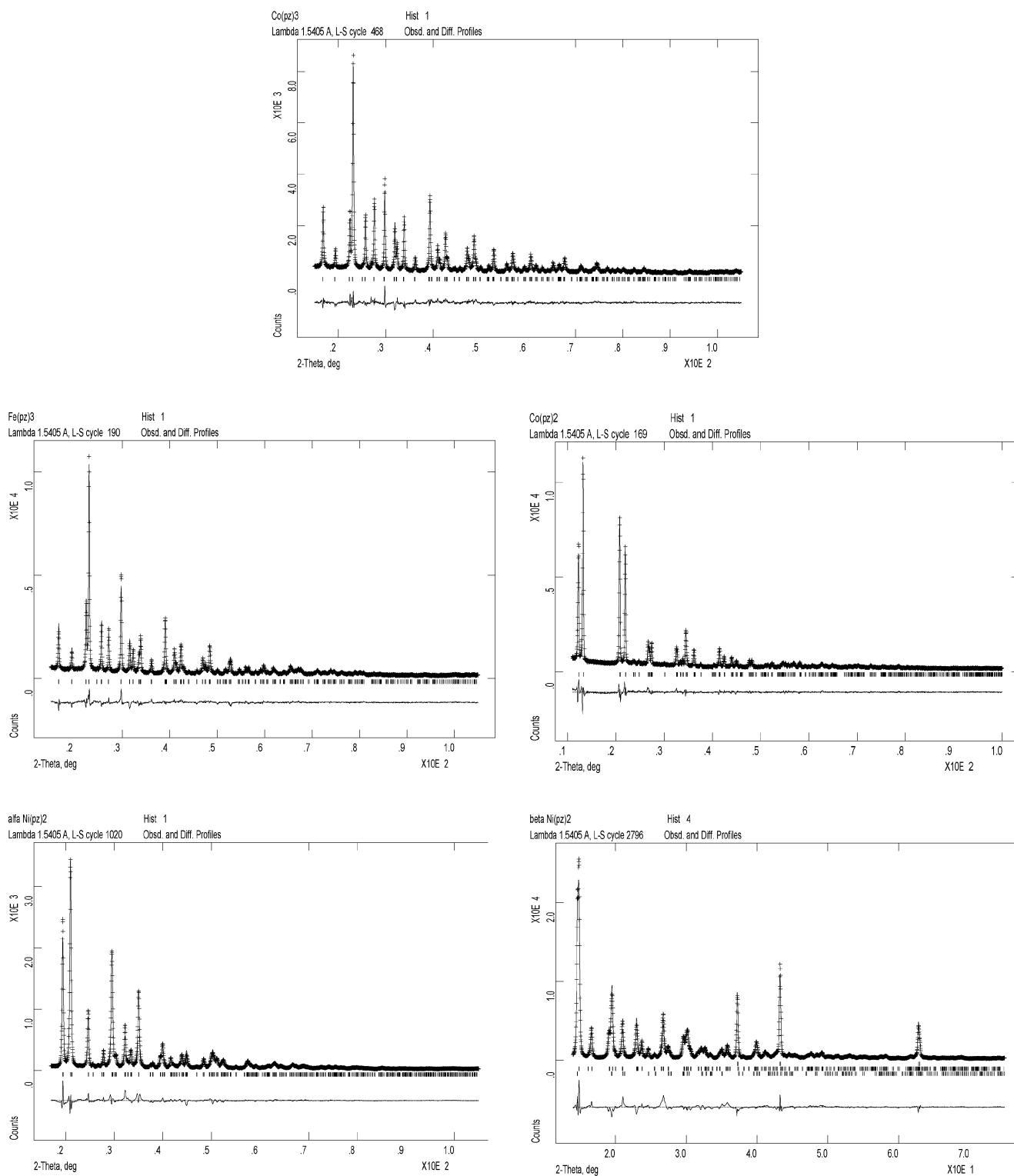
Figure 2. Rietveld refinement plots for Fe(pz)$_3$, Co(pz)$_2$, Co(pz)$_3$, α-Ni(pz)$_2$, and β-Ni(pz)$_2$, with difference plots and peak markers.

of the air-sensitive Fe(pz)$_2$ species (by reaction of ferrocene with molten pyrazole) has been very recently reported, and its crystal and molecular structures were determined, thanks to the fortunate isolation of a suitable single crystal.[18]

Generally speaking, the very poor solubility of such polymers typically prevents the growth of single crystals suitable for conventional diffraction studies; moreover, "wet" synthetic procedures have been often found to afford amorphous samples, preventing even a less conventional XRPD determination of their crystal and molecular structures. To circumvent this problem, a relatively high-temperature synthesis generally appears to be the obliged route to highly (micro)crystalline materials, as substantiated by several studies by others[18,29b] and us.[21a] Having this in mind, all metal

pyrazolates described in this paper were obtained (as microcrystalline powders) by reaction of the appropriate metal salt with pyrazole in refluxing *n*-butanol (140 °C), or, alternatively, by direct reaction with over-heated molten pyrazole (about 180 °C). In all cases, the starting materials have been chosen in order to take advantage of the basic nature of the anion (generally acetate or acetilacetonate, as well as oxide for nickel).

Cobalt. Cobalt(II) pyrazolate was obtained in a pure and crystalline form by reaction of pyrazole with cobalt(II) acetate in refluxing *n*-butanol (eq 1). Because of the deprotonating capability of the acetate anion, the formation of Co(pz)$_2$ proceeds without the necessity of external bases.

$$Co(CH_3COO)_2 + 2Hpz \rightarrow Co(pz)_2 + 2CH_3COOH \quad (1)$$
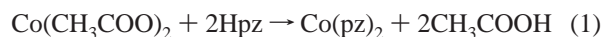
In a similar manner, Co(acac)$_3$ affords the Co(pz)$_3$ species. However, the XRPD studies have been carried out on samples synthesized in molten pyrazole, because of the higher crystallinity of these specimens, obtained at a higher temperature (ca. 180 °C). It is noteworthy that, when reaction 1 was carried out in a dioxygen atmosphere, analytically pure Co(pz)$_3$ was obtained, although in a poorer microcrystalline form. This oxidation reaction takes place only in the presence of free pyrazole (e.g., in the reaction medium); in the absence of Hpz, Co(pz)$_2$ appears to be quite stable toward oxidation. As further proof of its inert character, solid Co(pz)$_2$ was refluxed for 4 h in *n*-butanol under an O$_2$ atmosphere: the XRPD pattern of the resulting sample did not show any appreciable difference with respect to the freshly prepared specimen. This contrasts earlier observations on the poor stability of this polymer toward aerial oxidation.[29b]

Nickel. α-Ni(pz)$_2$ was obtained by reaction of Ni(II) acetate with pyrazole in *n*-butanol or, in absence of solvent, in molten pyrazole. Both routes afforded highly crystalline materials suitable for an XRPD study. It is noteworthy that, when NiO was employed in place of Ni(CH$_3$COO)$_2$, a different Ni(pz)$_2$ crystalline phase (β) was obtained. Any attempt to obtain this polymorph in a pure form miserably failed, the β-phase being inevitably contaminated by variable amounts of the α-phase and some residual nickel oxide. It is worthy to note that other preparations of a "generic" nickel(II) pyrazolate phase have been reported since 1977, starting from nickelocene,[30] nickel chloride or nitrate,[16] and nickel powder,[31] all lacking any experimental structural study. Presently, we have no clear explanation for the formation of the β-phase when using NiO instead of a number of other soluble (nickel chloride, sulfate, acetate) or insoluble [Ni(OH)$_2$, NiS] starting materials. The observation that transformation of α into β (or vice versa) cannot be achieved by heating (up to the decomposition temperature) or exposure to high pressure (with pellets left overnight at 2 GPa, which should favor the slightly denser β-phase) indicates that, differently from what observed in the Cu(pz) congeners,[21a] passing from one polymorph into the other requires the overcoming of a very high energetic barrier.

Iron. Fe(pz)$_3$ was obtained following the same synthetic route employed for the preparation of Co(pz)$_3$, exploiting the basic nature of the acetylacetonate anions in Fe(acac)$_3$.

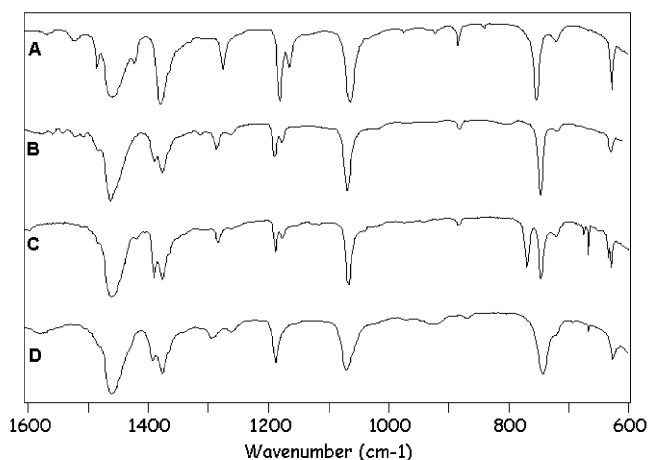**Figure 3.** IR spectra in the 1600−600 cm^{-1} region: A, Fe(pz)$_3$; B, Co-(pz)$_3$; C, α-Ni(pz)$_2$; D, Co(pz)$_2$.
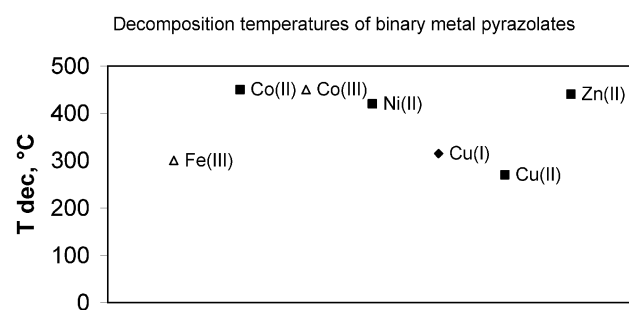

Figure 4. Decomposition temperatures for binary pyrazolates of the first transition metal series. The two polymorphs of Ni(pz)$_2$ possess comparable stability. The isomorphous bis(4-X-pyrazolate)copper(II) polymers (X = Cl, Br, and CH$_3$) decompose near 290 °C, thus behaving similarly to the parent Cu(pz)$_2$.

IR Spectroscopy. According to their nearly identical structural features (vide infra), IR spectra (Nujol mull, 3000−600 cm^{-1} region) of Co(pz)$_3$ and Fe(pz)$_3$ exhibit very similar patterns, showing only little differences in the position of the absorptions bands (see Experimental Section and Figure 3). Co(pz)$_2$, despite the different geometry around the metal centers, shows general features comparable with those of the Co(III) and Fe(III) derivatives. On the other hand, the square-planar geometry around the Ni(II) centers in α-Ni(pz)$_2$ causes a relatively more complex IR spectrum, with a clear splitting of the absorption related to C−H bending of the pyrazolate anion (see Figure 3).

Thermal Behavior. In agreement with earlier observations on analogue polyazaheterocyclic derivatives,[23] binary metal pyrazolates have been typically found to decompose without melting at rather high temperatures, up to ca. 450 °C in the most fortunate cases. Figure 4 shows a schematic plot of the measured decomposition temperatures (at ambient pressure) for the species presented in this paper and for the few known analogues.

Both Ni(pz)$_2$ phases exhibit thermochromism, because their powders, light yellow at −70 °C, progressively turn dark yellow (at RT) and deeply orange upon heating above 250 °C, this behavior being very rapid and completely reversible. Such observation, for a "generic" nickel(II) pyrazolate compound, had already been reported[33] and,
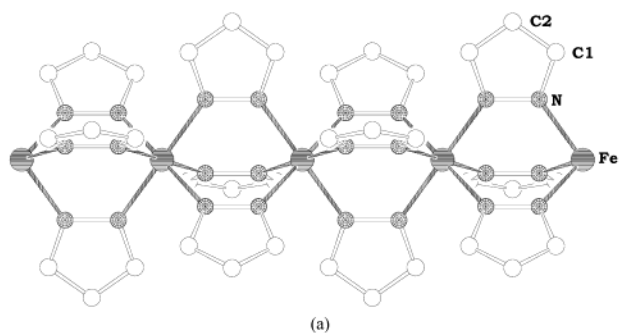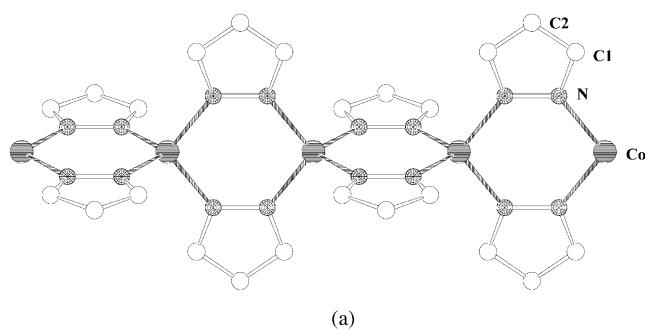
(a)
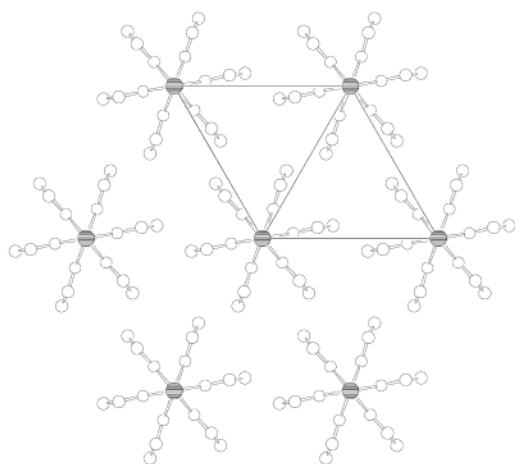
(b)

Figure 5. (a) Schematic drawing of the Fe(pz)$_3$ polymeric chain. Metal atoms in black, nitrogen atoms shaded, carbon atoms as empty spheres; hydrogen atoms omitted. (b) View of the hexagonal crystal packing down [001]. The isomorphous Co(pz)$_3$ species looks, at the drawing resolution, identical.

(a)

(b)

Figure 6. (a) Schematic drawing of the Co(pz)$_2$ polymeric chain. Metal atoms in black, nitrogen atoms shaded, carbon atoms as empty spheres; hydrogen atoms omitted. (b) View of the rectangular, pseudohexagonal, crystal packing down [001].

within this class of compounds, is not new: indeed, several Cu(4-Xpz)$_2$ species (X = H, Br, Me) are deeply thermochromic. In addition, two stable crystalline phases of Cu(4-Clpz)$_2$, possessing different (green and brown) colors, are known.[34] In the absence of structural characterization at high temperatures, but noting that both Ni(pz)$_2$ phases contain the same polymeric chain, we tentatively attribute their thermochromism to intramolecular effects, rather than to drastic changes in the "tertiary", i.e., supramolecular, structure.
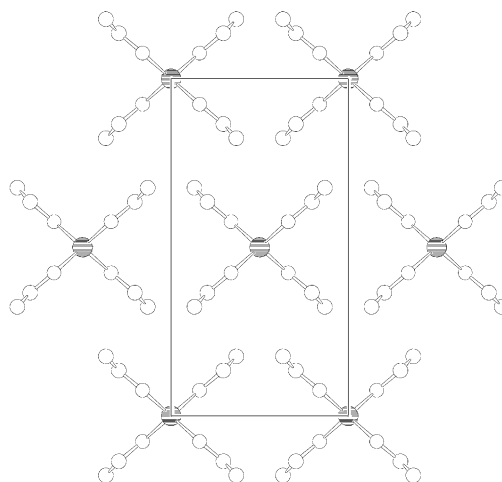
Crystal Structures of Fe(pz)$_3$ and Co(pz)$_3$. The two crystal structures, sharing space group symmetry and very similar features, are strictly isomorphous: chains of octahedrally coordinated M(III) ions run parallel to c, each M···M contact being bridged by three μ_2-pyrazolate ligands in the common *exo*-bidentate mode. Metal ions lie on -3 symmetry sites, while pyrazolates are bisected by a mirror plane passing through the carbon atom in the 4-position and the midpoint of the N−N vector. The shortest intermetallic contacts are 3.61 and 3.55 Å ($c/2$), while M−N bond distances are 1.98 and 1.95 Å, for Fe(pz)$_3$ and Co(pz)$_3$, respectively. A schematic drawing of the polymeric chain is depicted in Figure 5a, while Figure 5b shows the packing of the chains, as viewed down [001].

Crystal Structure of Co(pz)$_2$. Co(pz)$_2$ contains collinear chains of tetrahedrally coordinated metal ions (of 222 site symmetry), separated by bis(μ_2-pyrazolate) bridges (Co···Co 3.72 Å and Co−N 2.01 Å), running parallel to c. Also in the present case, pyrazolates act as *exo*-bidentate ligands and are bisected by crystallographic mirror planes. Comparison of the structural features of Co(pz)$_2$ with other known species indicates its isomorphous character with Cd(pz)$_2$,[21b] Cu(pz)$_2$,[35] Fe(pz)$_2$,[18] and, particularly, Zn(pz)$_2$, which shares almost identical lattice metrics and geometrical parameters.[21b] In all these strictly related crystal phases, the polymeric chains [depicted, for Co(pz)$_2$, in Figure 6a], of nearly cylindrical shape, pack in a centered rectangular fashion (Figure 6b); however, with being b only slighly different from $\sqrt{3}a$, a distorted hexagonal packing can be envisaged, characterized by an eccentricity value $|\epsilon|$ (defined in Table 2) of ca. 7%, the lowest among the species collected in Table 2. [A surprisingly low ϵ value, 0.4%, was found for Cd(pz)$_2$, which resulted in extreme accidental overlapping of diffraction peaks].[21b]

Crystal Structures of α- and β-Ni(pz)$_2$. Depending on the synthetic procedures described in preceding paragraphs,

(33) Trofimenko, S. *Chem. Rev.* **1972**, *72*, 497−509.

(34) Ehlert, M. K.; Rettig, S. J.; Storr, A.; Trotter, J. *Can. J. Chem.* **1991**, *69*, 432−439.

(35) Ehlert, M. K.; Rettig, S. J.; Storr, A.; Thompson, R. C.; Trotter, J. *Can. J. Chem.* **1989**, *67*, 1970−1974. Ehlert, M. K.; Storr, A.; Thompson, R. C.; Einstein, F. W. B.; Batchelor, R. *Can. J. Chem.* **1993**, *71*, 331−334.
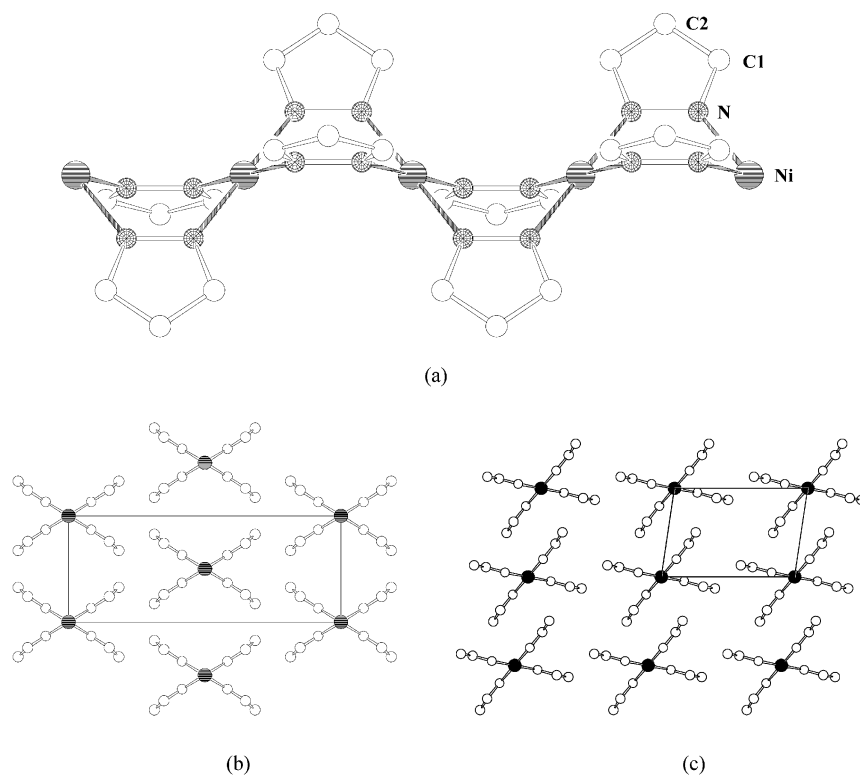
Figure 7. (a) Schematic drawing of the Ni(pz)$_2$ polymeric chain in the α-phase (identical, apart from numbering scheme, to that found in the β-phase). Metal atoms in black, nitrogen atoms shaded, carbon atoms as empty spheres; hydrogen atoms omitted. (b) View of the rectangular, pseudohexagonal, crystal packing of the α-phase down [001]. (c) View of the oblique, pseudorectangular, crystal packing of the β-phase down [010].

Ni(pz)$_2$ has been found to crystallize as different α (orthorhombic) and β (monoclinic) phases. In both crystal types, strictly collinear square-planar nickel atoms are present (Ni···Ni 3.47 and 3.49 Å, in α and β, respectively), linked by bis(μ_2-pyrazolate) bridges [Ni−N 1.87 Å]. The site symmetry of the pyrazolate ligands is again *m*, while nickel atoms, which in the β-phase are in general position, lie on −1 inversion centers in α. Within each chain (running parallel to *c* in α and *b* in β), the coordination planes of adjacent metals are not parallel but make a dihedral angle of about 73.7° (in both polymorphs), generating a wavy polymer (depicted in Figure 7a)[30] of much less isotropic cross section than those of the crystalline Fe(III), Co(III), and Co(II) species. These rods of "elliptical" section are expected to pack in a heavily distorted pseudohexagonal mode (as in α, Figure 7b) or to adopt a different packing type (oblique, but nearly rectangular, as in β, Figure 7c). Interestingly, the herringbone packing, observed in a number of organic polymers of anisotropic section, is not chosen in the present case. Even if a cyclic trimer of Ni$_3$(pz)$_6$ formula was suggested by Blake and co-workers,[30] none of the two Ni(pz)$_2$ phases is isostructural with the long known molecular Pt$_3$(pz)$_6$ species, with square-planar metal ions. The existence of a still uncharacterized Pt(pz)$_2$ polymer was also presented but was not further substantiated.[36]

Discussion

The polymers presented here, together with the few congeners reported in the recent literature, show that binary metal pyrazolates tend to afford highly crystalline species where strictly collinear chains of metal atoms are present. Some of these basic topologies of these chains are not new and can be related to the archetypic β-RuBr$_3$ (or anhydrous scandium acetate) and BeCl$_2$ phases [Fe(III)/Co(III) and Fe(II)/Co(II)/Cu(II)/Zn(II), respectively]; at variance, we are not aware of simple binary species adopting, in the solid state, the wavy chain structure of the polymers of both Ni(pz)$_2$ phases. The direct linkages of the metal centers may result in large cooperativity of magnetic interactions, as witnessed by the considerable hystereses found in a number of structurally related, but more complex, polymeric materials.[7,13]

Comparison of the refined M−N bond distances (see Table 2) clearly shows the expected trends: about 0.05 Å shorter values are found for M(III) versus M(II) species, while about 0.02 Å longer interactions are observed for iron versus cobalt isomorphous (octahedral or tetrahedral) species; this latter trend is further substantiated by the Cu−N value (1.96 Å) present in Cu(pz)$_2$ species. Moreover, the rather short (1.87 Å) Ni−N distance observed in α-Ni(pz)$_2$ agrees well with the relatively smaller ionic radius of square-planar Ni(II) ions. Inter alia, these results speak for a rather high reliability of the geometrical parameters derived from XRPD data of simple, highly (micro)crystalline, coordination polymers. While M···M contacts in the +3 ions well correlate with these apparent radii, this is not true for the tetrahedral M(II) species, where an extremely large Cu···Cu value of ca. 3.89

(36) Bürger, W.; Strähle, J. *Z. Anorg. Allg. Chem.* **1985**, *529*, 111−117.

Å and deformation from ideal symmetry of some of the MN_4 chromophores (D_{2d}, rather than T_d) are observed.

The anisotropic disposition of the metals in the crystal lattice suggests that the strongest electronic and, eventually, magnetic coupling in these systems are imputable to the polypyrazolate-bridged M···M contacts, rather than to interchain interactions, which might be at work only at very low temperatures. This is particularly true when substituted polyazoles and noncoordinating anions are used instead of the simple pyrazolate, the packing density of the polymers being lowered by side chains, anions, and, in some cases, solvent molecules. While a number of SC or ST polymers of this class have been prepared and studied for their interesting magnetic properties, their structural characterization has been but rarely performed; the model compounds reported here should partially fill the gap between polynuclear, but truly molecular, species of the appropriate ligands, and their polymeric counterparts, because it is expected that only small variations will occur by introducing noncoordinating organic residues, or other heteroatoms, in the 4-position.

The crystallographic results presented in the preceding description, summarized in Table 2, show a number of important structural features, shared by all, or most of, these species: (a) Pyrazolates, in their common *exo*-bidentate coordination mode, may afford double or triple bridges between metal ions which are about 3.4–3.9 Å apart, showing extreme versatility depending on the requirements of the ground-state electronic configuration at the metals. It is noteworthy that, in these pure end-members (which contain only one kind of metal ions in a well defined oxidation state), octahedral environments are found for d^5 and d^6 ions, tetrahedral geometry for d^6, d^7, d^9, and d^{10} ions, and square-planar coordination for d^8 centers. As a consequence, in a search for fine-tuning of the spectroscopic and magnetic properties of these polymers, it is possible to envisage partial metal substitution between isomorphous species [Fe(III)/Co(III); Fe(II)/Co(II)/Cu(II)/Zn(II)]. That such doping is chemically possible has already been proven in preliminary studies involving the Co(II) and Zn(II) ions,[16a] and in a number of related 1D and 2D polymers.[21,37] (b) The presence of methyls, or larger subtituents, in the 3 and/or 5 positions of the heterocycles is likely to disrupt the possibility of growing (ordered) polymeric species, because of the interactions of residuals belonging to (poly)azolates bound onto adjacent metals. Indeed, polymeric species have been observed only for the 4-substitution (with halides, methyls[34] or even much larger residues), while species containing 3,5-dimethylpyrazolates have been invariably found as cyclic or "truncated" linear oligomers.[38] Moreover, recent results on 3,5-diterbutylpyrazolates (b₂pz) on a number of main group and transition metal ions have definitely assessed the importance of steric hindrance driving toward the less common η^2-*N,N-endo*-bidentate mode in mononuclear M(b₂-pz)$_n$ complexes.[39] (c) The accessibility of a tetrahedral "excited state" for Ni(II), obtained, for example, by forcing this geometry in the crystals of a magnetically diluted Ni$_x$Zn$_{1-x}$(pz)$_2$ phase (x = small) or by doping magnetically active [Fe/Co/Cu](pz)$_2$ polymers, could generate mixed-metal phases with interesting responses, determined by the amount of distortion (different for each metal, and amplified by the lattice constraints and periodicity), dopant level, and internal redox propensity[40] for one-electron transfer between adjacent metals. A similar, but complementary, approach has been developed by Kahn and co-workers, who optimized the ST thermal hysteresis loop by doping the [Fe(1,2,4-triazole)₃](ClO₄)₂·nH₂O polymer with small amounts of 4-aminotriazole.[7]

The unsubstituted pyrazolate ligands tend to lie on crystallographic mirror planes, with the metal ions in high symmetry environments; thus, the overall complexity of the "macromolecular chains" is deeply buried within the crystal lattice, making the stereochemical description of the metal and of their bonds to the heterocycles quantitatively reliable, because most uncertainties deriving from the use of XRPD are annihilated by the accurately determined lattice parameters.

Conclusions

The structure determination of simple metal-organic polymers from single crystals or even from powder diffraction data is a fundamental step toward the interpretation of many relevant chemical, spectroscopic, and magnetic data. That this step cannot be overlooked is clear from repeated claims on the structural properties inferred from ancillary, but nonexhaustive, techniques (see for example the erroneous assessment of the stereochemistry or the connectivity of simple metallorganic polymers such as [Ru(CO)₄]$_n$[41] or [PdCl(acetonyl)]$_n$[42]), mostly because solid-state spectroscopies suffer from subtle "packing" effects hiding what would be self-consistent evidence in solution chemistry.

In the present case, we have definitely assessed the stereochemistry of several coordination polymers, whose basic structures were already inferred from those of related oligomeric species (mostly containing neutral polyazoles and suitable counterions). For this class of compounds, several reports have shown that simple building rules can result in a number of unprecedented crystal structures and topology,[22b,23] with the wide existence of polymorphic species of even different dimensionality, thus requiring control and the knowledge of the resulting species as fundamental steps toward the achievement of tailored properties. In addition, the dichotomy bewteen cyclic or extended species for Ni(pz)₂ has been solved in an unexpected manner, by detecting the

(37) Lawandy, M. A.; Huang, X.; Wang, R.-J.; Li, J.; Lu, J. L.; Yuen, T.; Lin, C. L. *Inorg. Chem.* **1999**, *38*, 5410−5414.

(38) Ehlert, M. K.; Rettig, S. J.; Storr, A.; Thompson, R. C.; Trotter, J. *Can. J. Chem.* **1990**, *68*, 1494−1498. Ehlert, M. K.; Rettig, S. J.; Storr, A.; Thompson, R. C.; Trotter, J. *Can. J. Chem.* **1993**, *71*, 1425−1436. Rettig, S. J.; Storr, A.; Summers, D. A.; Thompson, R. C.; Trotter, J. *Can. J. Chem.* **1997**, *75*, 949−958.

(39) Gust, K. R.; Knox, J. E.; Heeg, M. J.; Schlegel, H. B.; Winter, C. H.; *Angew. Chem., Int. Ed.* **2002**, *41*, 1591−1594.

(40) Ayers, T.; Scott, S.; Goins, J.; Caylor, N.; Hathcock, D.; Slattery, S. J.; Jameson, D. L. *Inorg. Chim. Acta* **2000**, *308*, 7−12.

(41) Masciocchi, N.; Moret, M.; Cairati, P.; Ragaini, F.; Sironi, A. *J. Chem. Soc., Dalton Trans.* **1993**, 471−475.

(42) Masciocchi, N.; Ragaini, F.; Sironi, A. *Organometallics* **2002**, *21*, 3489−3492.

(43) De Wolff, P. M. *J. Appl. Crystallogr.* **1968**, *1*, 108−113.

(44) Smith, G. S.; Snyder, R. L. *J. Appl. Crystallogr.* **1979**, *12*, 60−65.

presence of two distinct crystallographic phases containing (only) the infinite polymer.